

Forward electron emission in collisions of He^{2+} ions with Ar atoms with simultaneous capture of two electrons

L. Sarkadi* and D. Nagy

*Institute for Nuclear Research of the Hungarian Academy of Sciences (MTA Atomki),**P.O. Box 51, H-4001 Debrecen, Hungary*

(Received 29 August 2016; published 31 October 2016)

The energy spectrum of the electrons ejected in forward direction from Ar atoms with simultaneous bound-state capture of two electrons has been measured by impact of 30 keV/amu He^{2+} ions with the aim to clarify the discrepancy between the results of two previous experiments concerning the existence of the cusp-shaped peak for electrons with velocity close to the ion velocity. A peak structure has been observed which is dominated by a broad cusp attributed to the zero-energy electron emission in the projectile-centered reference system at the 2^3S excitation threshold of He^0 . Further narrower peaks have been identified as results of the decay of autodetachment resonant states of He^- populated during the collision by three-electron bound-state capture.

DOI: [10.1103/PhysRevA.94.042709](https://doi.org/10.1103/PhysRevA.94.042709)

I. INTRODUCTION

This work was motivated by the contradictory results of two experiments carried out for the electron emission from collisions of energetic He^{2+} ions with Ar atoms. In both experiments the double electron capture with simultaneous target ionization (DCI) was investigated by measuring the double differential cross section (DDCS) for the process as a function of the electron energy and emission angle. The first experiment was made in 2000 by Fregenal *et al.* [1] using 25 keV/amu $^3\text{He}^{2+}$ ions. The authors identified the DCI channel by detecting coincidences between the electrons and the neutralized outgoing projectiles. At 0° they observed a narrow symmetric cusp-shaped structure for electrons emitted with velocity v_e close to the ion velocity v_p .

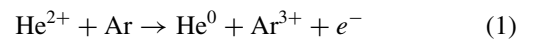
The second experiment was carried out by Zhang *et al.* [2] in 2014 at slightly higher impact energy, 30 keV/amu. It was a triple coincidence experiment. Applying the COLTRIMS (cold target recoil ion momentum spectroscopy) measuring technique, the electrons were detected in coincidence with the charged-state analyzed outgoing projectiles and the recoil target ions separated according to their charge. The DCI electron spectrum at 0° measured by Zhang *et al.* did not show the cusp-shaped peak.

The existence of the cusp peak for neutral outgoing projectiles is an interesting question considering the threshold character of the cusp formation. The $v_e \approx v_p$ electrons emitted from the collision in the forward direction fly with very small velocity in the projectile-centered reference system. The low-energy electron states around the projectile may be populated by the target ionization, via the “electron capture to the continuum” (ECC) process [3]. Because of the dominant role of the electron-projectile interaction, the cusp formation is governed by the universal two-body threshold laws derived by Wigner [4]. According to these laws, cusp is expected to occur only for projectiles interacting with an attractive, long-range force.

For neutral atomic projectiles the interaction has short range, i.e., the ECC cusp should not exist. Quite unexpectedly,

Sarkadi *et al.* [5] observed an intense and narrow ECC cusp in 75 keV/amu He^0 on He, Ar collisions. To explain the observation, Barrachina [6] proposed a final-state interaction (FSI) model in which he assumed the formation of a virtual (i.e., zero-energy) resonance state of the $(e^- + \text{He}^0)$ system. Such a negative ion state exists at the 2^1S excitation threshold of He^0 . The mechanism predicted by the model has been verified in a series of subsequent experiments [7–9]. Furthermore, cusp was found also in the measurements of the transfer ionization (TI) that leads neutral projectile in the final state for He^+ projectile ion [5,10,11].

The measurement of the DDCS for the three-electron DCI induced by He^{2+} ions in Ar



represents a challenge for the experimentalists, partly because of its expected small value, and partly due to the presence of unwanted (unphysical) electron emission processes leading also to He^0 in the final state. The latter have two categories: (i) electron emission associated with the He^+ and He^0 fractions (contaminants) of the primary He^{2+} beam; (ii) electron emission due to double collisions. The main sources of the beam contamination are the interaction of He^{2+} ions with the residual gas of the measuring chamber and the scattering of the ions at the edges of the collimator apertures. The He^+ and He^0 contaminants contribute to the measured coincidences by electron emission via TI and pure target ionization, respectively. As far as the double collisions are concerned, the following two processes have important contributions, particularly regarding the cusp electron production: (i) double electron capture in the first collision and pure target ionization in the second collision by the neutralized projectile; (ii) TI in the first collision and single electron capture by the outgoing He^+ ion in the second collision.

According to Zhang *et al.* [2] the cusp observed by Fregenal *et al.* [1] is a result of the above “background” processes, i.e., an artifact of their experiment. Zhang *et al.* excluded the existence of the DCI cusp on the basis of the potential-energy levels of the $[\text{HeAr}]^{2+}$ quasimolecule presented by Moretto-Capelle *et al.* [12], namely that the population of the $\text{He}(1s^2) + \text{Ar}^{3+}$ channel is much more likely energetically

*sarkadil@atomki.hu

than the $\text{He}(1s nl, n \geq 2) + \text{Ar}^{3+}$ channel, and thereby the formation of the virtual resonance at the 2^1S threshold can be ruled out.

The aim of the present work was to decide the question of the existence of the cusp-shaped peak in the energy spectrum of the electrons emitted from the process (1) in forward direction.

II. EXPERIMENTAL METHOD

The measurements were performed at the 1.5 MV Van de Graaff accelerator of Atomki. The experimental setup was an upgraded version of the arrangement that had been applied in a previous investigation of the electron cusp [13]. The He^{2+} ions, produced by interaction of the He^+ beam of the accelerator with the residual gas of the beam channel, were selected from the original ion beam with a four-stage electrostatic charge-state selector [14]. A collimator with a length of 45 cm defines the final He^{2+} beam of 0.75 mm diameter.

The electron ejected from the interaction of the ion beam and an effusive Ar gas target in forward direction is reflected by an electrostatic mirror [15] into backward angles ($\approx 160^\circ$), while the projectile passes through the mirror. The reflected electron flies through a drift tube and is then detected by a channel electron multiplier. The outgoing projectile ion is charge-state analyzed by means of an electrostatic deflector and detected by an ion detector [16]. The energy of the electron is determined from the time-of-flight of the electron, obtained as the difference between the arrival time of the electron and that of the ion. The time difference was measured by an FPGA based time-to-digital converter developed in Atomki. The time resolution was 5 ns.

The upgrade of the time-of-flight (TOF) system consisted of improving its energy and angular resolution by replacing the drift tube by a three times longer one. Furthermore, in the tube we built in a five-element electrostatics lens for focusing, accelerating, or decelerating the electrons. The TOF system was operated with a modest energy resolution of 4%. The acceptance (half) angle was 1.5° . The base pressure in the collision chamber was 1.5×10^{-6} mbar.

We made the experiment at 30 keV/amu, i.e., at the energy of the experiment of Zhang *et al.* The DCI process (1) was identified by detecting the electrons in coincidence with the outgoing neutralized projectiles. The coincidence yield was very small; the measurements took altogether 75 h. The DCI electron spectrum showed the cusp; however, it was a question whether it is not only experimental artifact. Therefore, we made systematical measurements to eliminate the contributions of the above-discussed background processes. To determine the contributions of the He^+ and He^0 contaminants to the DCI coincidence yield, first we measured their fractions in the He^{2+} beam without the target gas. We obtained the following values: $f(\text{He}^+) = (1.6 \pm 0.2)\%$ and $f(\text{He}^0) = (0.23 \pm 0.04)\%$. Then in separate experiments made with He^+ and He^0 beams we measured the electron yield for the processes

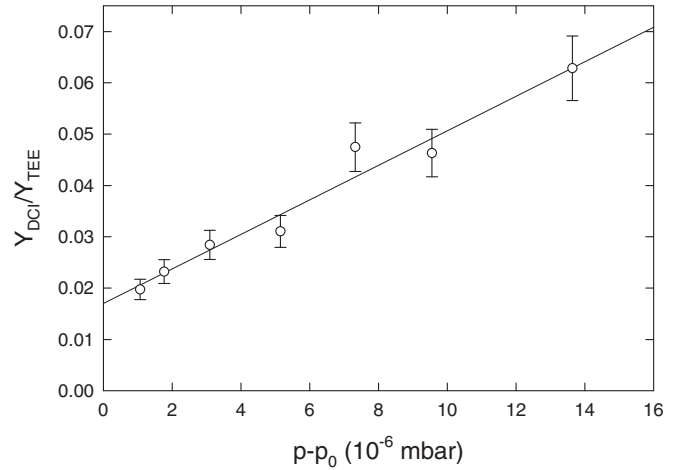


FIG. 1. Ratio of the yield of the electrons produced in the DCI process (1) and that of the total electron emission as a function of the target gas pressure.

by coincident detection of the electrons with the outgoing He^0 projectiles. These measurements and that for the DCI process (1) were repeated at several values of the target gas pressure. By taking into account the fractions of the contaminant ions, the contributions of the above processes were subtracted from the DCI coincidence yield at each pressure value. Furthermore, the DCI yield measured at zero target pressure was also subtracted. At the lowest pressure the latter yield was about 40% of the total DCI yield; the contribution of the beam contaminants was only 10%.

We measured also the yield of the total electron emission (TEE) by detecting coincidences between the electrons and the outgoing ions of all the charge states. In Fig. 1 we plotted the ratio of the DCI and TEE yield, $Y_{\text{DCI}}/Y_{\text{TEE}}$, as a function of the target gas pressure, $p - p_0$. Here Y_{DCI} and Y_{TEE} are integrated electron yields over the energy in the peak region, and p_0 is the pressure of the residual gas. The figure demonstrates the presence of the double collisions. In the lack of double collisions both DCI and TEE would depend linearly on the pressure; therefore, their ratio would be constant. TEE is not affected by double collisions; we found that it depended linearly on the pressure. The linear increase of the $Y_{\text{DCI}}/Y_{\text{TEE}}$ ratio with the pressure is explained by the quadratic pressure dependence of the double collisions contributing to the DCI yield.

As is seen from the figure, $Y_{\text{DCI}}/Y_{\text{TEE}}$ is finite at zero target gas pressure. It is a small value: the contribution of DCI to the total electron production is less than 2%. The finite value, however, does not mean that the peak exists. The existence of the peak can be proved by point-by-point extrapolation of the energy spectra measured at different pressure values to zero pressure (see, e.g., Ref. [17]). To do this, first we divided the spectral DCI yields by $p - p_0$, and then at each electron energy point of the spectra belonging to the different pressure values we fitted the pressure dependence with a straight line (see Fig. 2), and constructed the zero target pressure spectrum as the intercepts of these lines. *Relative* DDCS was obtained by correcting the extrapolated spectrum for the transmission and detection efficiency of the TOF system. Our result, presented

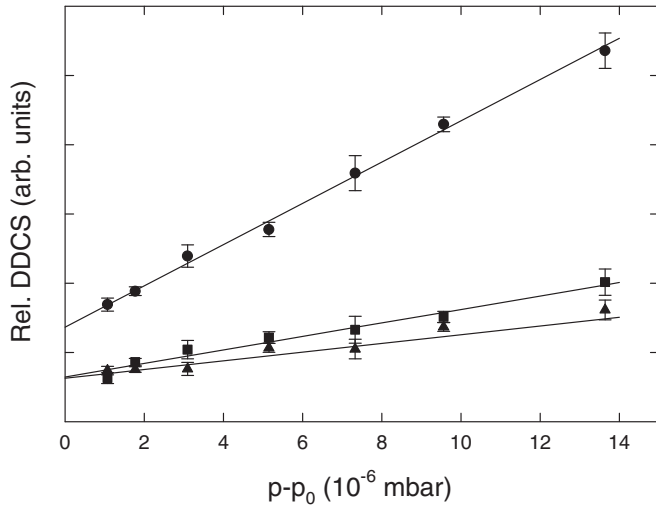


FIG. 2. Examples of the extrapolation of the points of the energy spectrum to zero pressure at three selected electron energies: 13.3 eV (squares), 16.8 eV (circles), and 19.2 eV (triangles).

in Fig. 3, shows a peak at $v_e = v_p$, thus supporting the observation of Fregenal *et al.* [1].

The DCI spectrum obtained in the present work cannot be compared directly with that measured by Fregenal *et al.* because of the difference in the impact energies, 30 keV/amu and 25 keV/amu, respectively. However, considering that the forward electron emission is dominantly governed by the electron-projectile interaction, one expects that the two spectra become comparable by transforming the electron energy to the relative velocity between the electron and the projectile, $v'_e = v_e - v_p$. In Fig. 4 we plotted the two spectra as a function of v'_e . By normalizing the spectra at a point below the maximum (at $v'_e = -0.035$), an excellent agreement was obtained in their shapes except around $v'_e \approx 0$ where the spectrum of Fregenal *et al.* is peaked more sharply as a result of the two data

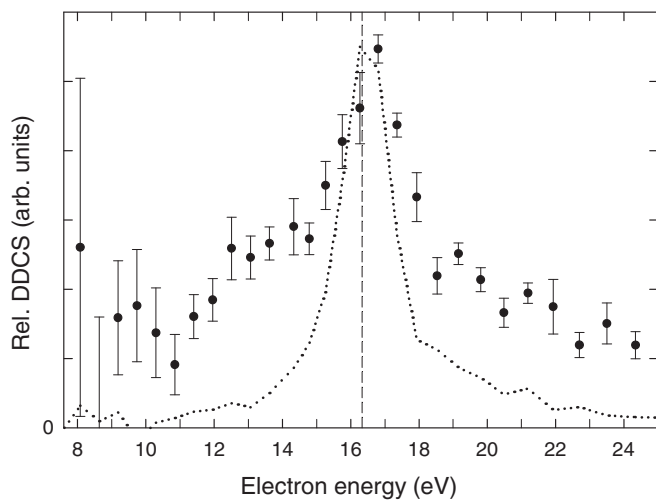


FIG. 3. DCI spectrum extrapolated to zero target gas pressure (circles with error bar). The dotted line represents the spectrum measured for process (3). The two spectra are normalized at their maxima.

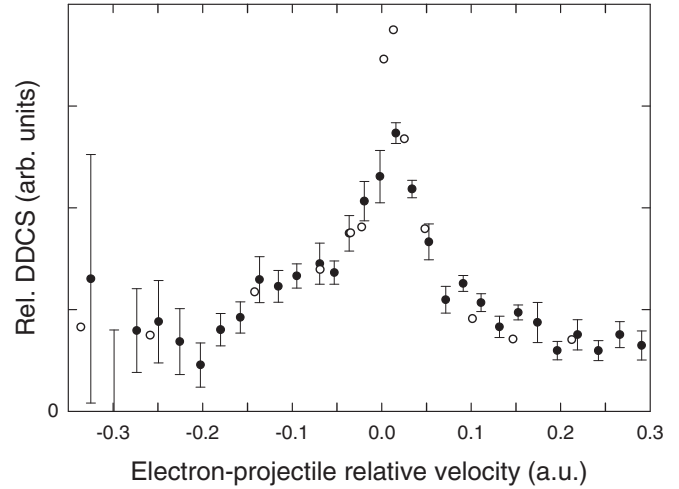


FIG. 4. Comparison of the DCI spectrum obtained in the present work (closed circles with error bar) with that measured by Fregenal *et al.* [1] (open circles).

points of highest intensity. As a possible explanation of the narrower central part of the spectrum, one cannot exclude the contribution of the background processes discussed in the Introduction [particularly process (3)] due to the beam contamination and the double collisions in the measurements Fregenal *et al.* At the same time, some difference in the spectrum shape is also expected due to the dependence of the DCI process on the impact energy.

III. RESULTS AND DISCUSSION

Looking for the origin of the DCI cusp, it is plausible to assume the same mechanism as that of the ECC cusp formation for neutral He projectile: the capture of the three electrons into He^{2+} may populate the virtual state of He^- lying at the 2^1S threshold of He^0 . To check this assumption, in Fig. 3 we plotted also the ECC peak measured by He^0 impact in process (3). According to the figure, the ECC peak is much narrower than the DCI peak. This means that the virtual state probably does not play a role in the DCI cusp formation.

The DCI peak in Fig. 3 even seems to have a structure: a narrower peak superimposed on a broader peak. The same structure can be observed also in the spectrum measured by Fregenal *et al.* (see Fig. 4). Searching further for the origin of the DCI cusp, we assumed that the broad component is produced by the same mechanism as that proposed to explain the ECC cusp observed by Báder *et al.* [9] at the impact of a 400 keV He^0 beam in pure 2^3S metastable state. The latter authors attributed the broad cusp to a threshold effect known to exist in the formation of the He^- resonance states, namely to that caused by the proximity of the 2^2S ($1s2s^2$) resonance at the 2^3S threshold of He^0 [18,19].

Because of the poor counting statistics of the DCI spectra measured at the various gas pressures, the point-by-point extrapolation could be made only by increasing the original energy bin of the measurements by a factor of four. Even in this case the error bars of the points of the extrapolated spectrum were too large for a detailed analysis. Instead, for the latter purpose we summed the spectra taken at the three

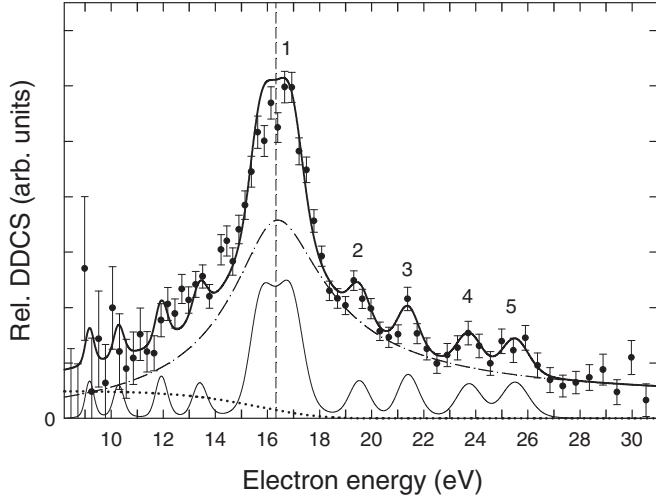


FIG. 5. Sum of the DCI spectra measured at the lowest three pressure values (circles with error bars). The notations of the curves are as follows. Thick solid line, the result of the model calculation based on Eqs. (4) and (5); dashed-dotted line, the contribution of the zero-energy electron emission occurring at the 2^3S threshold of He^0 ; thin solid line, the contribution due to the decay of He^- resonance states; dotted line, the contribution of the nonresonant DCI process.

lowest pressure values. In this way we obtained a spectrum of better quality.

The summed spectrum is shown in Fig. 5. It consists of a central narrow peak on the top of a broad peak. Further peaks at the high-energy wing of the broad peak are also visible. Assuming that the latter originate from the decay of autodetachment resonant states of He^- , they are expected to appear symmetrically with respect to 16.3 eV, the energy corresponding to $v_e = v_p$. However, because of the rapid decrease of the transmission of the TOF system below 14 eV, the counting statistics was not enough to establish the existence of the low-energy counterparts of the peaks.

We note that the He^- autodetachment transition leading to the peak at 19.6 eV in the spectrum (peak 2) has already been observed in the experiment carried out by Báder *et al.* [9] using a 400 keV 2^3S He^0 beam. The 19.6 eV energy corresponds to 0.15 eV in the projectile reference frame. This transition appeared in the ECC spectrum measured by Báder *et al.* at both wings of the cusp, at around 49 and 59 eV. This strongly supports our assumption that the peaks in the summed spectrum are due to autodetachment transitions of He^- .

The parameters of the transitions corresponding to the peaks in the spectrum (relative strength, energy, width) were estimated by the following model calculations. Considering the sharp angular distribution of the electron emission, a spectrum point at energy E_0 is obtained as an average of the DDCS over the detection solid angle $\Delta\Omega$:

$$Y(E_0) = \frac{1}{\Delta\Omega} \int_{\Delta\Omega} \int_{\Delta E} \frac{d^2\sigma}{dE d\Omega} g(E - E_0) d\Omega dE. \quad (4)$$

The convolution over the energy range of the measurement ΔE in Eq. (4) takes into account the energy resolution. The spectrometer function $g(E - E_0)$ was approximated by a Gaussian.

$d^2\sigma/dE d\Omega$ was obtained by transforming the projectile-centered DDCS, $d^2\sigma/dE'd\Omega'$, to the laboratory system. For the sake of simplicity we considered isotropic electron emission following the decay of the He^- resonance states. $d^2\sigma/dE'd\Omega'$ was assumed to depend on the electron energy E' in the projectile frame as

$$\frac{d^2\sigma}{dE'd\Omega'} \propto C_{2^1S} F_{2^1S}(E') + C_{2^3S} F_{2^3S}(E') + \sum_i C_i L_i(E'). \quad (5)$$

Here $F_{2^1S}(E')$ and $F_{2^3S}(E')$ are the so-called enhancement factors that describe the zero-energy electron emission at the 2^1S and 2^3S thresholds of He^0 [20,21], and $L_i(E')$ are Lorentzian functions that account for the peaks due to the decay of the He^- resonance states. The C_{2^1S} , C_{2^3S} and the C_i coefficients, as well as the positions and width of the Lorentzian peaks are free parameters of the model.

By varying the free parameters we fitted the spectrum predicted by the model to the measured spectrum. The result is shown in Fig. 5. A good fit was obtained with $C_{2^1S} \approx 0$, confirming the assumption that the virtual resonance at the 2^1S threshold of He^0 does not contribute to DCI. On the contrary, the contribution related to the 2^3S threshold is large, and it provides an excellent description of the broad peak component of the measured spectrum at higher energies. At lower energies a good fit was achieved by assuming direct DCI electron emission.

As a further result of the fitting, we attributed the central narrow peak (peak 1) to the decay of the $(1s2p2p')^4P^e$ shape resonance of He^- [22–24] to the 2^3P state of He. The transition energy and the width of this resonance ($\Delta E_r = 10.80 \pm 0.07$ meV and $\Gamma = 7.16 \pm 0.07$ meV, respectively [25]) were kept constant during the fitting.

For peak 2 the results of the fitting in the projectile frame are $\Delta E_r = 0.15 \pm 0.01$ eV and $\Gamma = 10 \pm 5$ meV. The peak may be attributed to the He^- resonance observed by Brunt *et al.* [26] in their measurements of the cross section for excitation of metastable states of He by electron impact. The resonance marked by the authors as “R-S feature” in the excitation function at 22.88 eV decays to the $1s3s^3S$ state with energy $\Delta E_r = 0.161$ eV. According to Brunt *et al.* the width of the resonance is $\Gamma = 18$ meV, which is larger than that observed in the present work.

For peak 3 the fitting yielded $\Delta E_r = 0.35 \pm 0.02$ eV and $\Gamma = 10 \pm 5$ meV. The peak may originate from the decay of a He^- resonance lying just above the 3^3P level of He, at 23.06 eV [26–29]. The energy of the transition to the $1s3s^3S$ state is $\Delta E_r = 0.342$ eV. In their review paper, Buckman and Clark [30] recommended a width value of 32 meV for this resonance, which is again larger than that observed in the present work. This discrepancy and also that found for peak 2 is partly explained by the relatively large energy width of the electron beams (typically 20 meV), and partly by the excitation of more overlapping resonances in the electron-impact experiments. The theoretical calculations of Freitas *et al.* [31] predict four resonances ($^2F^o$, $^2P^o$, $^2D^e$, $^2G^e$) in a narrow energy range between 23.02 and 23.07 eV. One may assume that in ion-atom collisions only one of the above resonances is excited.

The energies of the peaks 4 and 5 in the projectile reference system are 0.70 ± 0.03 eV and 1.03 ± 0.03 eV, respectively. The width of both peaks is limited by the energy resolution; it cannot be larger than 20 meV. We note that for a good overall fit of the spectrum we had to include peaks 4 and 5, but due to the poor statistics their existence is uncertain. Even if they exist, the large number of He^- resonance states that contribute to this part of the spectrum (configurations $1s nl n'l'$ with $n, n' \geq 4$) do not allow their unambiguous identification.

IV. CONCLUSIONS

In summary, we have measured the energy spectrum of the electrons ejected from Ar atoms at 0° by impact of 30 keV/amu He^{2+} ions under the condition of simultaneous double electron capture. In contrast to the recent measurements by Zhang *et al.* [2], the spectrum shows a maximum for electrons with velocity close to the ion velocity. In addition, we have observed a peak structure. The structure is dominated by a broad cusp attributed to the zero-energy electron emission due to the proximity of the 2S ($1s2s^2$) resonance at the 2^3S threshold

of He^0 . Further peaks have been identified as results of the decay of autodetachment resonant states of He^- .

Our result supports the explanation given by Szótér [32] for the cusp electron production by impact of neutral He atoms. Szótér's idea is based on the formation and decay of intermediate resonant states of He^- leading to low-energy electron emission in the projectile frame. The importance of the present work lies in that it demonstrates that, unlike for He^0 , for He^{2+} projectiles such states can be populated in a wide variety by the capture of three electrons. The latter process is not limited by strict selection rules; therefore, the study of the resulting electron emission by means of the zero-degree electron spectroscopy may open an alternative way to explore the He^- resonance states, as compared to the traditional methods based on the electron scattering on He, or photodetachment of He^- [19,30,33].

ACKNOWLEDGMENT

This work was supported by the National Scientific Research Foundation (OTKA, Grant No. K109440).

-
- [1] D. Fregenal, J. Fiol, G. Bernardi, S. Suárez, P. Focke, A. D. González, A. Muthig, T. Jalowy, K. O. Groeneveld, and H. Luna, *Phys. Rev. A* **62**, 012703 (2000).
- [2] R. T. Zhang, X. Ma, S. F. Zhang, X. L. Zhu, W. T. Feng, D. L. Guo, Y. Gao, B. Li, D. B. Qian, H. P. Liu, S. Yan, and P. Zhang, *Phys. Rev. A* **89**, 032708 (2014).
- [3] J. Macek, *Phys. Rev. A* **1**, 235 (1970).
- [4] E. P. Wigner, *Phys. Rev.* **73**, 1002 (1948).
- [5] L. Sarkadi, J. Pálinkás, Á. Kövér, D. Berényi, and T. Vajnai, *Phys. Rev. Lett.* **62**, 527 (1989).
- [6] R. O. Barrachina, *J. Phys. B: At., Mol., Opt. Phys.* **23**, 2321 (1990).
- [7] M. Kuzel, L. Sarkadi, J. Pálinkás, P. A. Závodszy, R. Maier, D. Berényi, and K. O. Groeneveld, *Phys. Rev. A* **48**, R1745 (1993).
- [8] L. Sarkadi, M. Kuzel, L. Víkor, P. A. Závodszy, R. Maier, D. Berényi, and K. O. Groeneveld, *Nucl. Instrum. Methods, B* **124**, 335 (1997).
- [9] A. Báder, L. Sarkadi, L. Víkor, M. Kuzel, P. A. Závodszy, T. Jalowy, K. O. Groeneveld, P. A. Macri, and R. O. Barrachina, *Phys. Rev. A* **55**, R14 (1997).
- [10] L. Víkor, L. Sarkadi, J. A. Tanis, A. Báder, P. A. Závodszy, M. Kuzel, K. O. Groeneveld, and D. Berényi, *Nucl. Instrum. Methods, B* **124**, 342 (1997).
- [11] L. Sarkadi, L. Lugosi, K. Tőkési, L. Gulyás, and Á. Kövér, *J. Phys. B: At., Mol., Opt. Phys.* **34**, 4901 (2001).
- [12] P. Moretto-Capelle, D. Bordenave-Montesquieu, A. Bordenave-Montesquieu, and M. Benhenni, *J. Phys. B: At., Mol., Opt. Phys.* **31**, L423 (1998).
- [13] L. Sarkadi and A. Orbán, *Phys. Rev. Lett.* **100**, 133201 (2008).
- [14] Á. Kövér, L. Sarkadi, J. Pálinkás, D. Berényi, Gy. Szabó, T. Vajnai, O. Heil, K. O. Groeneveld, J. Gibbons, and I. A. Sellin, *J. Phys. B: At., Mol., Opt. Phys.* **22**, 1595 (1989).
- [15] L. Sarkadi and A. Orbán, *Meas. Sci. Technol.* **17**, 84 (2006).
- [16] A. Báder, L. Sarkadi, Gy. Hegyesi, L. Víkor, and J. Pálinkás, *Meas. Sci. Technol.* **6**, 959 (1995).
- [17] L. Víkor, P. A. Závodszy, L. Sarkadi, J. A. Tanis, M. Kuzel, A. Báder, J. Pálinkás, E. Y. Kamber, D. Berényi, and K. O. Groeneveld, *J. Phys. B: At., Mol., Opt. Phys.* **28**, 3915 (1995).
- [18] J. R. Taylor, *Scattering Theory* (Wiley, New York, 1972).
- [19] G. J. Schulz, *Rev. Mod. Phys.* **45**, 378 (1973).
- [20] R. O. Barrachina, *Nucl. Instrum. Methods, B* **124**, 198 (1997).
- [21] P. A. Macri and R. O. Barrachina, *J. Phys. B: At., Mol., Opt. Phys.* **31**, 1303 (1998).
- [22] J. R. Peterson, Y. K. Bae, and D. L. Huestis, *Phys. Rev. Lett.* **55**, 692 (1985).
- [23] P. A. Závodszy, L. Sarkadi, L. Víkor, and J. Pálinkás, *Phys. Rev. A* **50**, R899 (1994).
- [24] L. Víkor and L. Sarkadi, *Phys. Rev. A* **55**, R2519 (1997).
- [25] C. W. Walter, J. A. Seifert, and J. R. Peterson, *Phys. Rev. A* **50**, 2257 (1994).
- [26] J. N. H. Brunt, G. C. King, and F. H. Read, *J. Phys. B: At. Mol. Phys.* **10**, 433 (1977).
- [27] F. M. J. Pichanick and J. A. Simpson, *Phys. Rev.* **168**, 64 (1968).
- [28] L. Sanche and G. J. Schulz, *Phys. Rev. A* **5**, 1672 (1972).
- [29] S. J. Buckman, P. Hammond, F. H. Read, and G. C. King, *J. Phys. B: At. Mol. Phys.* **16**, 4039 (1983).
- [30] S. J. Buckman and C. W. Clark, *Rev. Mod. Phys.* **66**, 539 (1994).
- [31] L. C. G. Freitas, K. A. Berrington, P. G. Burke, A. Hibbert, A. E. Kingston, and A. L. Sinfailam, *J. Phys. B: At. Mol. Phys.* **17**, L303 (1984).
- [32] L. Szótér, *Phys. Rev. Lett.* **64**, 2835 (1990).
- [33] T. Andersen, *Phys. Rep.* **394**, 157 (2004).